Supplement of Atmos. Chem. Phys., 23, 2613–2625, 2023
https://doi.org/10.5194/acp-23-2613-2023-supplement

Atmospheric Chemistry and Physics
Open Access

Supplement of

Technical note: Chemical composition and source identification of fluorescent components in atmospheric water-soluble brown carbon by excitation–emission matrix spectroscopy with parallel factor analysis – potential limitations and applications

Tao Cao et al.

Correspondence to: Jianzhong Song (songjzh@gig.ac.cn)

Contents:

S1. Sample information

S1.1. BrC model compounds

To more accurately identify the chemical characteristics of fluorescent components and answer the question that which and how much light-absorbing species can be detected by the excitation-emission matrix (EEM) method, 35 organic compounds with strong light absorption were tested. These organic compounds were usually detected in ambient samples (e.g., aerosols, rain water, and cloud, and combustion-derived particulate matter) and selected as the typical BrC model compounds. According to the chemical composition and structures, these compounds are classified into phenolic compounds, aromatic acids, nitroaromatic compounds, protein-like compounds, N-heterocyclic compounds, and polycyclic aromatic hydrocarbons (PAHs) (Table S1). These organic compounds all contain aromatic π-π conjugate structures and have the potential to produce fluorescence and make contribution to atmospheric fluorophores. They include:

(i) Phenolic compounds: as reported in literatures, plenty of phenolic compounds can be emitted from biomass burning and coal combustion and were also with high concentration in atmospheric environment, such as in aerosol, cloud and fog water (Sengupta et al., 2020; Smith et al., 2014; Yu et al., 2014; Yu et al., 2016). In the present study, six phenol and their derivatives were selected, which are phenol, catechol, hydroquinone, 2-methoxyphenol, vanillin and 4-hydroxyacetophenone.

(ii) Aromatic acids: aromatic acids were mainly produced from biomass burning and atmospheric photochemical reactions, which were usually detected in ambient aerosol, cloud water and rainwater (Li et al., 2020; Santos et al., 2019; Sharp et al., 2021). In this study, nine benzoic acids and its derivatives were tested, including benzoic acid, phthalic acid, terephthalic acid, trimesic acid, 2-hydroxybenzoic acid, 4-hydroxybenzoic acid, 4-hydroxy-3,5-dimethoxybenzoic acid, 3,5-dihydroxybenzoic acid and vanillic acid.

(iii) Nitroaromatic compounds (NACs): NACs refer to substances containing at least one nitro (NO_2) on the aromatic ring, such as nitrophenols and their derivatives (Chow et al., 2016). Nitrophenols were believed to be mainly derived from biomass combustion and secondary chemical reactions of phenols (such as the addition of NO_3 radical), and they were the important chromophores in atmospheric BrC (Bai et al., 2020; Huang et al., 2021; Lin et al., 2016; Wang et al., 2017; Yuan et al., 2020), which accounted for 50-80% of total solvent extractable BrC absorption at more than 400 nm (Huang et al., 2021; Lin et al., 2017). In our study, six NACs compounds included 4-nitrophenol, 4-nitrocatechol, 3,4-dinitrophenol, 2-methoxy-5-nitrophenol, 2-nitrobenzaldehyde, and 2-nitronaphthol were chosen and tested by EEM.

(iv) Protein-like compounds: Amino acids were the basic structural constituent of protein and peptides in organisms and also an important component in the fluorescent chromophores of natural organic matter (Coble, 1996; Murphy et al., 2013). They were usually identified in cloud water and aerosols, but with relative low concentrations (Bianco et al., 2014; Bianco et al., 2016; Song et al., 2017; Zhang and Anastasio, 2003). In this study, three amino acids with aromatic structures, tryptophan, tyrosine, and phenylalanine were tested.

(v) N-heterocyclic compounds: These compounds can be produced from combustion of biomass and fossil fuels and secondary atmospheric reactions with NO_x, which were usually identified in ambient aerosol and cloud/fog water (Jiang et al., 2019; Kosyakov et al., 2020) (Ackendorf et al., 2017; Lian et al., 2022). In our study, pyridine, pyrrole, imidazole, and imidazole-2-formaldehyde were selected as the typical heterocyclic compounds and tested by EEM.

(vi) Polycyclic aromatic hydrocarbons (PAHs): PAHs, a class of compounds with two or more aromatic rings in their structure, are also the important chromophores in atmospheric aerosols because of their large conjugated structure (Huang et al., 2021; Huang et al., 2020; Lin et al., 2017; Mahamuni et al., 2020). In the present study, seven PAHs and its derivatives compounds are tested: naphthalene, phenanthrene, pyrene, 9-fluorenone, anthraquinone, 1-Naphthol, and 2-naphthalenecarboxylic acid.

It is noted that imidazole-2-formaldehyde exhibit different light absorption ability at different pH (Ackendorf et al., 2017). In order to straightly show that different classified compounds contain this property or not as well as imidazole-2-formaldehyde, different types of compounds (phenol, catechol, 4-hydroxyacetophenone, tryptophan and imidazole-2-formaldehyde) were also tested at different pH (pH = 2, 5, 8). These five compounds exhibited similar fluorescence peak location except for imidazole-2-formaldehyde (Figure S2). In addition, we also measured the fluorescence spectra for organic compounds with different mixing ratios. Results indicated that the fluorescence peak overlap with each other, but the fluorescence peak position does not change (Figure S3), which are similar with the results as reported by previous study (Andrade-Eiroa et al., 2013) and indicated that the fluorescence peaks of target compounds were not significantly changed even it mixed with other organic compounds.

S1.2. Primary combustion source samples

Thirteen primary combustion-derived particulate samples were selected in this study, included six biomass burning (BB), five coal combustion (CC), and two vehicle emission (VE) samples (Figure S3). The six BB samples include three crop straw samples (rice straw, wheat straw and corn straw) and three wood samples (pine, Chinese fir and White poplar). Five CC samples, were collected from the combustion of four bituminous coal (C-1, C-2, C-3 and C-4) and one anthracite coal: (C-5). These smoke samples are all collected in a laboratory furnace, and the details of the experimental methods have been described elsewhere (Cao et al., 2021). Two VE samples were collected from 2 types of vehicles, including emission samples of medium-duty diesel trucks (China V diesel vehicles) and gasoline cars (China VI gasoline vehicles) (Tang et al., 2020). All the samples were stored in a −20 ℃ refrigerator before analysis.

S1.3. Soil and purified fulvic and humic acid samples

Soils are important contribution of fulvic and humic substance and also a significant primary source of ambient aerosols. In this study, 5 soil samples were taken from the agriculture areas of Guangdong province, China, include Soil 1-5.

After collection, these soil samples were air drying and sealed in dark environment.

In addition, fulvic acid (FA) and humic acid (HA) are usually considered as important contribution to atmospheric WSOM (Chen et al., 2020). In our study, six FA and HA samples were kindly provided by Professor Weilin Huang from Rutgers university, include Suwannee river FA, Orchard FA and Pearl river FA; Chalsea HA, Aldrich HA, and Pahokee peat HA, were also studied in this study.

S1.4. $PM_{2.5}$ samples

The ambient $PM_{2.5}$ samples were collected from Guangzhou (GZ) and Chuzhou (CZ) of China, respectively. The GZ site is located at the campus of Guangzhou Institute of Geochemistry, CAS, which near the downtown of Guangzhou city and represent urban area. The CZ site is situated in the campus of Anhui Science and Technology University, which has emission sources from agricultural production, biomass burning, and other anthropogenic activities and is a typical suburban area. Daily aerosol samples were collected on quartz fiber filter membranes from April 6 to 22, 2021, totally 34 ambient aerosol samples were obtained. The sampling instrument is high-flow $PM_{2.5}$ sampler (JCH-1000H, Juchuang Environmental Protection Group Co., Ltd., Shandong, China) with a sampling flow of 1.0 m^3/min. The quartz fiber filter membranes are prebaked at 450 ℃ for 5 hour to remove the impure organics. The samples are collected and stored in a refrigerator at - 20 ℃ for further analysis.

In addition, 43 sample of $PM_{2.5}$ samples were also collected from February 1, 2018 to January 22, 2019 at GZ site. Each sample collection lasted for 24 h and time interval was set as 7 days. These samples were grouped as wet (April to September) and dry (October to March) season $PM_{2.5}$. The sampling instruments and work condition were same as above.

S2. Standard solution preparation and extraction methods for WSOM

Solutions of the BrC model organic compounds were prepared by dissolving a certain amount of dried solids or liquids in Milli-Q water or methanol. Ultrasonic agitation is used for both preparations in order to get a complete dissolution. Naphthalene, phenanthrene, pyrene, 2-naphthalenecarboxylic acid and anthraquinone were difficult dissolved in water, so methanol was used as solvent (Chen et al., 2020).

The ambient aerosol, combustion-derived particle, and soil samples were treated as follow: certain amounts of sample were ultrasonic extracted with ultrapure water in a 50 mL glass tube for three times. Then the supernatant was filtered with 0.22 μm PTFE syringe filter (CNW, ANPEL Laboratory Technologies (Shanghai) Inc., China) to obtain water-soluble organic matter extracts.

S3. Carbon contents, UV spectra, and chemical analysis

The concentration of water-soluble organic carbon (WSOC) in water extracts were determined by a total organic carbon (TOC) analyzer (TOC-VCPH analyzer, Shimadzu, Kyoto, Japan). The UV-visible absorption spectra of all samples were recorded between the wavelengths of 200 to 700 nm using a UV-2600i spectrophotometer (Shimadzu, Kyoto, Japan). The sample solution was placed in a 1-cm quartz cuvette and analyzed at 1 nm intervals. Ultrapure water (or methanol) was used as a blank reference for the samples and the spectra are corrected by the instrument and operating blanks.

Then the optical parameters, such as absorption Ångström exponent (AAE, 330-400nm) and mass absorption efficiency at 365 nm (MAE_{365}), were calculated based on previous studies (Cao et al., 2021; Fan et al., 2020). The calculation equation of AAE and MAE_{365} were described as follows:

$$A_\lambda = \mathrm{K}\lambda^{-AAE}$$

where A_λ is the absorbance at wavelength λ (330-400nm), and K is a constant.

$$\mathrm{MAE}_\lambda = \frac{A_\lambda}{c \cdot l} \times \ln(10)$$

where A_λ is the absorbance at λ nm (365nm used here), c is the organic carbon concentration of targets in solution (μgC mL^{-1}), and l is the absorbing path length (0.01 m).

In addition, the water soluble inorganic species (NO_3^-, SO_4^{2-}, Cl^-, NH_4^+, K^+, Na^+, Ca^{2+}, Mg^{2+}) in ambient aerosols were measured with a Dionex ICS-900 ion chromatography system (Thermo Fisher Scientific, USA) as described previously (Huang et al., 2020).

S4. EEM and PARAFAC analysis

The EEM fluorescence spectra of the solution samples in a 1 cm quartz cuvettes were recorded by a three-dimensional fluorescence spectrophotometer (Aqualog, HORIBA Scientific, USA) at room temperature. The scanning ranges for excitation (Ex) and emission (Em) was 200–500 nm and 250-550 nm, respectively. The wavelength increments of the excitation and emission scans were both 5 nm. The ultrapure water was used as blank references and calculated Raman peak area. In addition, absorbance measurements were used to correct the EEM for inner-filter effects (IFEs) according to the previous studies if the absorbance was higher than 0.05 at 250 nm (Fu et al., 2015; Murphy et al., 2013). Raman and Rayleigh scattering was removed by subtracting Milli-Q water spectra and insert zero value to the Raman and Rayleigh scattering region (Stedmon and Bro, 2008; Murphy et al., 2013). Background samples were also analyzed, and the background values were subtracted from all sample result. To avoid concentration effects, the fluorescence spectra were normalized by the Raman peak of water and the OC concentration of WSOC; and the specific fluorescence intensities (RU/(mgC/L)) are shown (Yang et al., 2022).

The PARAFAC modeling procedure was conducted in MATLAB by the drEEM toolkit (Murphy et al., 2013; Murphy et al., 2018). The PARAFAC was computed using two to nine component models, with non-negativity constraints and a residual analysis; and split half analysis was used to validate the number of fluorescence components. According to the results of the split-half and core consistency analysis, three component models were chosen for further analysis. The identified individual fluorophores were compared with online database OpenFluor (based on the identified fluorophores in nature organic matter and the similarity of results for both excitation and emission wavelength were set at 98%, Murphy 2013). The relative contribution of individual chromophores was estimated by calculating the maximum fluorescence intensities (F_{max}: maximum fluorescence intensity of identified fluorescence components, relative content % = $F_{max}/\Sigma F_{max}$) (Cao et al., 2021; Chen et al., 2020; Matos et al., 2015).

Moreover, the EEM parameter, humification index (HIX) was also calculated and compared in this study. The humification index (HIX). HIX were described as the ratio of integral area of Em wavelength from 435-480 nm and 300-345 nm where Ex =254 nm. (Qin et al., 2018; Yang et al., 2022). The fluorescence volumes (FVs) of the WSOC samples were calculated based on the EEM matrix in the excitation wavelength of 230-450 nm and emission wavelength of 250-550 nm. The FVs was then normalized by the OC concentration of these samples, yielding the normalized fluorescence volumes (NFV)(RU-nm^2-[mg/L]$^{-1}$OC) (Chen et al., 2020).

Table S1. Chemical and optical properties of the selected BC model compounds

	Compounds	Molecular formula	Structure	The normalized UV-vis spectra
Phenolic compounds	Phenol	C_6H_6O	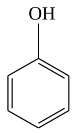	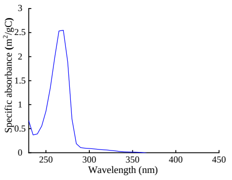
	Catechol	$C_6H_6O_2$	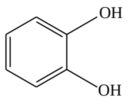	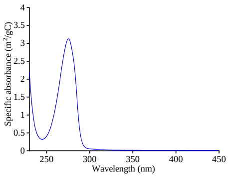
	Hydroquinone	$C_6H_6O_2$	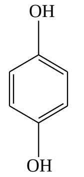	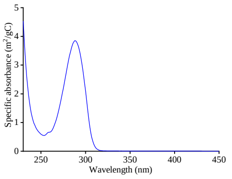
	2-Methoxyphenol	$C_7H_8O_2$	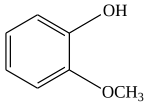	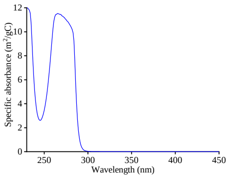
	Vanillin	$C_8H_8O_3$	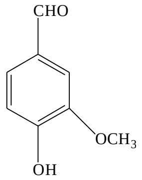	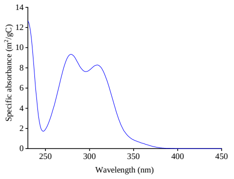
	4-Hydroxyacetophenone	$C_8H_8O_2$	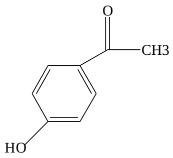	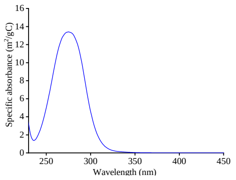
Aromatic acid	Benzoic acid	$C_7H_6O_2$	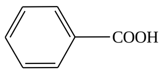	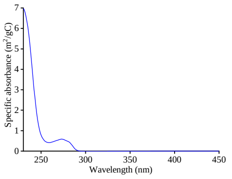
	Phthalic acid	$C_8H_6O_4$	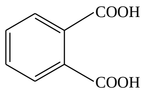	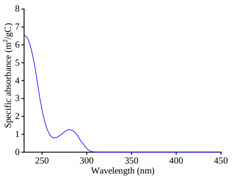

Aromatic acid	Terephthalic acid	$C_8H_6O_4$	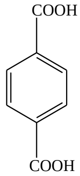	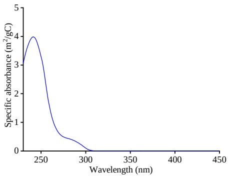
	Trimesic acid	$C_9H_6O_6$	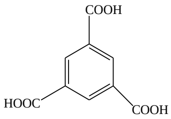	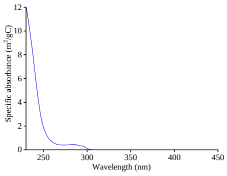
	2-Hydroxybenzoic acid	$C_7H_6O_3$	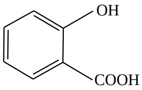	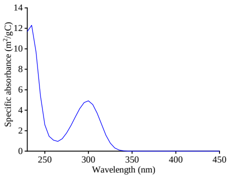
	4-Hydroxybenzoic acid	$C_7H_6O_3$	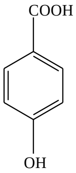	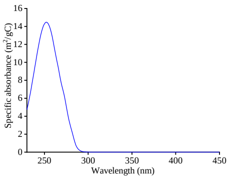
	4-Hydroxy-3,5-dimethoxybenzoic acid	$C_9H_{10}O_5$	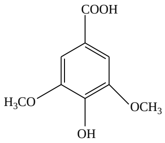	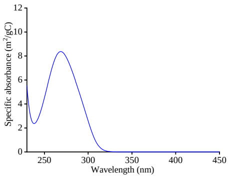
	3,5-Dihydroxybenzoic acid	$C_7H_6O_4$	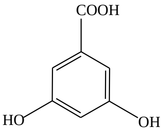	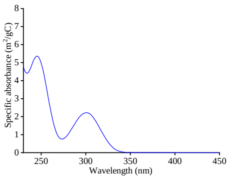
	Vanillic acid	$C_8H_8O_4$	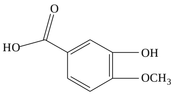	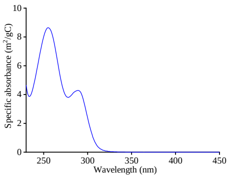
Nitroaromatic compounds	4-Nitrophenol	$C_6H_5NO_3$	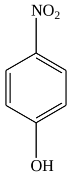	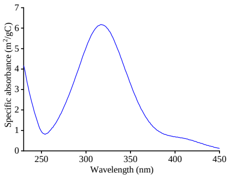
	4-Nitrocatechol	$C_6H_5NO_4$	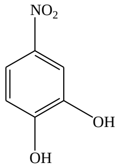	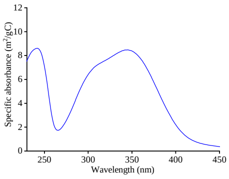

Nitroaromatic compounds	3,4-Dinitrophenol	$C_6H_4N_2O_5$	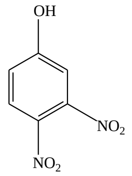	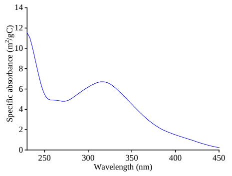
	2-Methoxy-5-nitrophenol	$C_7H_7NO_4$	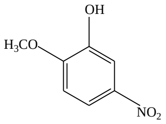	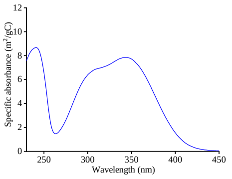
	2-Nitrobenzaldehyde	$C_7H_5NO_3$	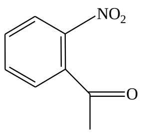	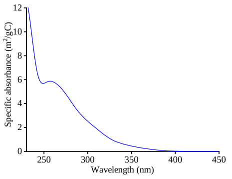
	2-Nitronaphthol	$C_{10}H_7NO_3$	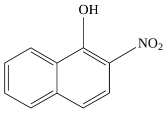	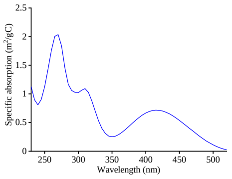
Protein-like compounds	Tryptophan	$C_{11}H_{12}N_2O_2$	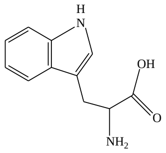	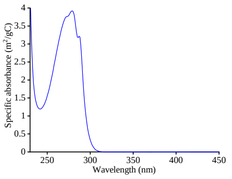
	Tyrosine	$C_9H_{11}NO_3$	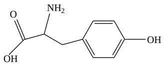	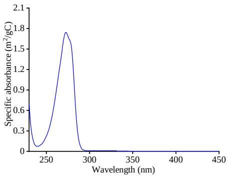
	Phenylalanine	$C_{10}H_{13}NO_2$	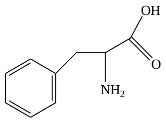	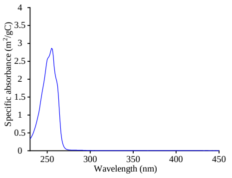
N-heterocyclic compounds	Pyridine	C_5H_5O	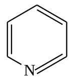	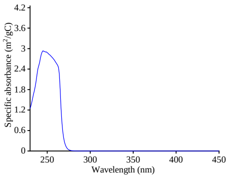
	Pyrrole	C_4H_5N	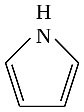	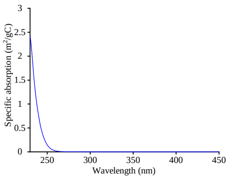

N-heterocyclic compounds	Imidazole	$C_3H_4N_2$	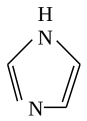	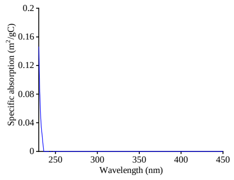
	Imidazole-2-formaldehyde	$C_4H_4N_2O$	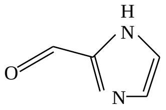	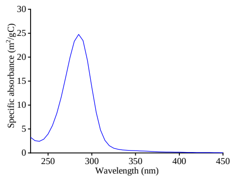
Polycyclic aromatic hydrocarbons	Naphthalene	$C_{10}H_8$	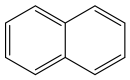	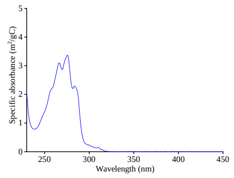
	Phenanthrene	$C_{14}H_{10}$	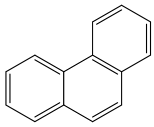	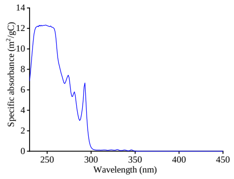
	Pyrene	$C_{16}H_{10}$	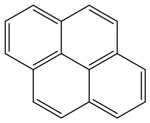	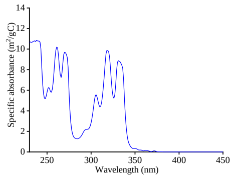
	9-Fluorenone	$C_{13}H_8O$	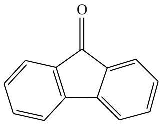	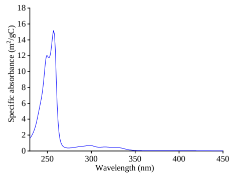
	Anthraquinone	$C_{14}H_8O_2$	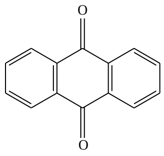	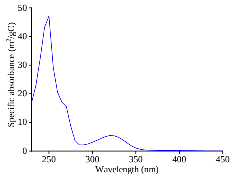
	1-Naphthol	$C_{10}H_8O$	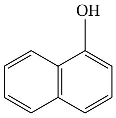	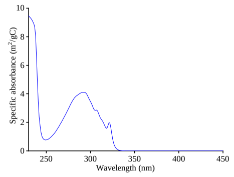
	2-Naphthalenecarboxylic acid	$C_{11}H_8O_2$	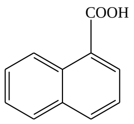	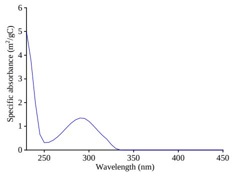

Table S2. Detail information of absorption and fluorescence properties of model BrC compounds

Compounds	Fluorescent location (Ex/Em)	The normalized Fluorescence intensity (R.U./(mgC/L))	Log (NFV) (RU-nm^2-[mg/L]$^{-1}$ OC)	Ambient concentration (aerosols)	References
Phenol	270/295	0.48	4.65	5-100*10^{-6} M (cloud and fog water)	(Smith et al., 2014)
Catechol	275/310	0.12	4.34		
Hydroquinone	270/320	0.34	6.43		
2-methoxyphenol	275/310	0.21	4.62	5-100*10^{-6} M (cloud and fog water)	(Smith et al., 2014)
Vanillin				0.1-100 ng/m^3	(Vione et al., 2019)
4-hydroxyacetophenone					
Benzoic acid	270/300	0.08	3.68	5*10^{-6} M (rain water)	(Santos et al., 2019)
Phthalic acid				4.77 ng/m^3	(Shen et al., 2018)
Terephthalic acid				46.84 ng/m^3	
Trimesic acid				9.45ng/m^3	(Kitanovski et al., 2014)
2-Hydroxybenzoic acid	230, 290/400	0.88	5.33	0.6μg/m^3	(Li et al., 2020)
4-Hydroxybenzoic acid	255/320	0.03	3.41	1.1 ng/m^3	(Teich et al., 2019)
4-Hydroxy-3,5-dimethoxybenzoic acid	260/330	0.25	4.44		
3,5-Dihydroxybenzoic acid	230/355	0.14	4.13		
Vanillic acid	250,280/320	0.29	5.76	0.1-100 ng/m^3	(Vione et al., 2019)
4-Nitrophenol				7.0 ng/m^3	(Ikemori et al., 2019)
4-Nitrocatechol	240/330	0.02	3.41	6.8 ng/m^3	
3,4-Dinitrophenol				4*10^{-3} ng/m^3	(Teich et al., 2017)
2-Methoxy-5-nitrophenol					

Table S2 Continued

Compounds	Fluorescent location (Ex/Em)	The normalized Fluorescence intensity (R.U./(mgC/L))	Log(NFV) (RU-nm^2-[mg/L]$^{-1}$ OC)	Ambient concentration (aerosols)	References
2-Nitrobenzaldehyde					
2-Nitronaphthol					
Tryptophan	275/350	0.77	4.96	26 pmol/m^3 (aerosol); 5.63*10^{-7} M (cloud water)	(Bianco et al., 2016; Zhang and Anastasio, 2003)
Tyrosine	270/300	0.82	4.44	31 pmol/m^3(aerosol); 4.5*10^{-8} M (cloud water)	
Phenylalanine	255/280	0.19	3.67	29 pmol/m^3(aerosol); 3.37*10^{-7} M (cloud water)	
Pyridine					
Pyrrole					
Imidazole					
Imidazole-2-formaldehyde	310/460	0.36	5.25	4 ng/m^3	(Ackendorf et al., 2017)
Naphthalene	275/330	9.1	4.83	3.09-11 ng/m^3	(Yang et al., 2006)
Phenanthrene	250/350,365	1.95	4.36	1.97-5.72 ng/m^3	
Pyrene	240,265,330/370, 390	0.33	4.49	1-6 ng/m^3	(Zhang et al., 2021)
9-Fluorenone	280/340	0.06		3.26 ng/m^3	(Lee et al., 2012)
Anthraquinone			3.62	143 pg/m^3	(Castells et al., 2003)
1-Naphthol	230,290/460	1.47	5.32	3-9 pg/m^3	(Ma et al., 2016)
2-Naphthalenecarboxylic acid	230,280/370	6.3	5.84		

Table S3. Comparison results of four independent fluorophores identified by PARAFAC analysis

Component 1	Component 2	Component 3	Sources of component	References
EX=235/270 nm, EM=330nm	EX=235/320nm, EM=390nm	EX=250/355nm, EM=455nm		
Protein-like and non-N-containing species	Less oxygenated species	Highly oxygenated species	Ambient aerosol	Chen et al 2016; 2021
Small molecular size compounds; SVOCs; naphthalene-like	SOA from biogenic and anthropogenic VOCs	High molecular weight from biomass burning,	Ambient aerosol	Wang et al., 2020
Peak B and T; protein-like	Peak A and M; Marine humic-like or humic-like	Peak C; Humic-like	ambient aerosol / Marine water	Fu et al., 2015; Coble et al., 1996
Polyphenols or low molecular PAHs;	Secondary formation from burning (oxidized phenols) or high molecular PAHs	Aromatic compounds/ Fulvic acid	Ambient aerosol	This study

(a) Phenolic compounds

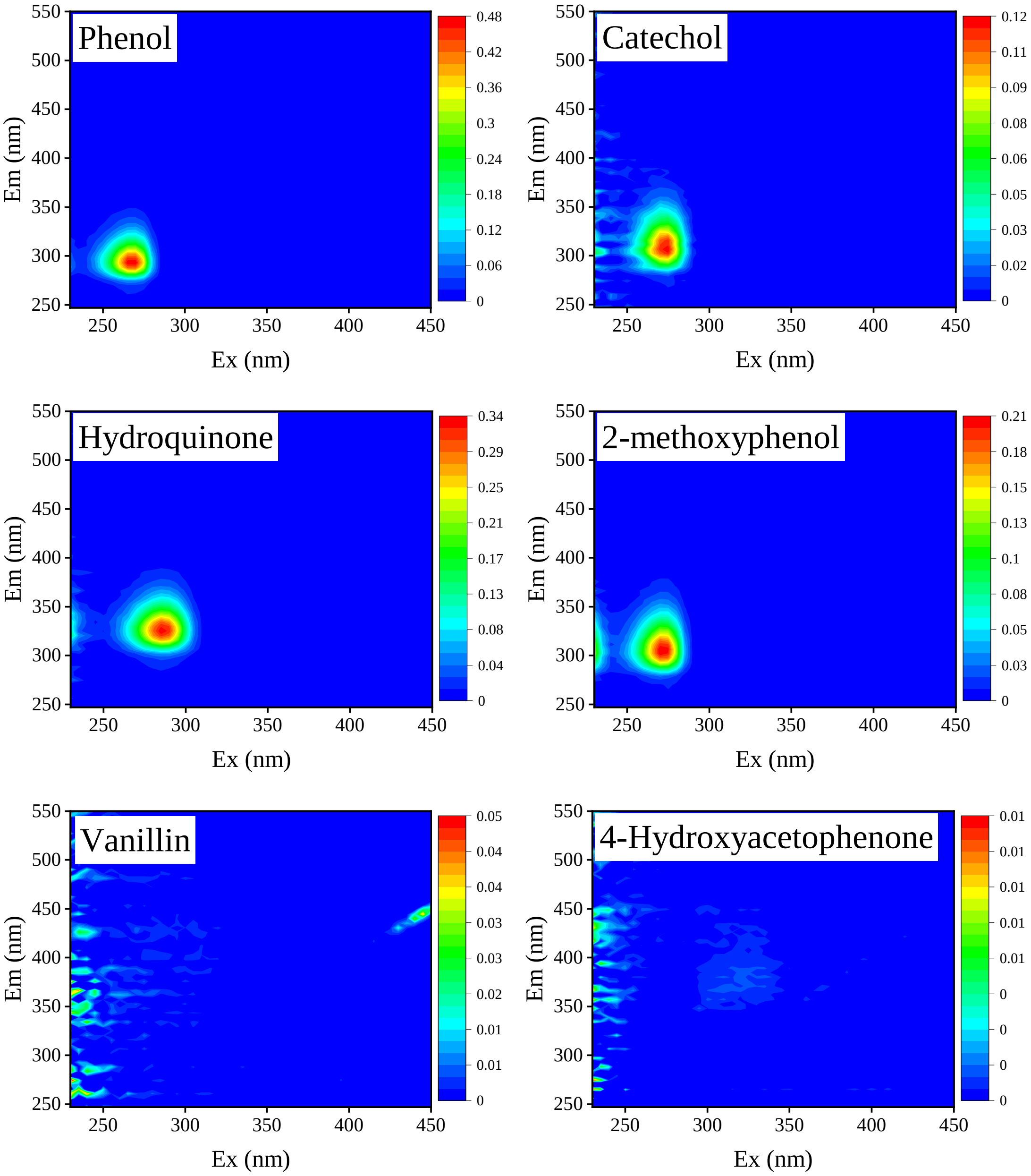

(b) Aromatic acid

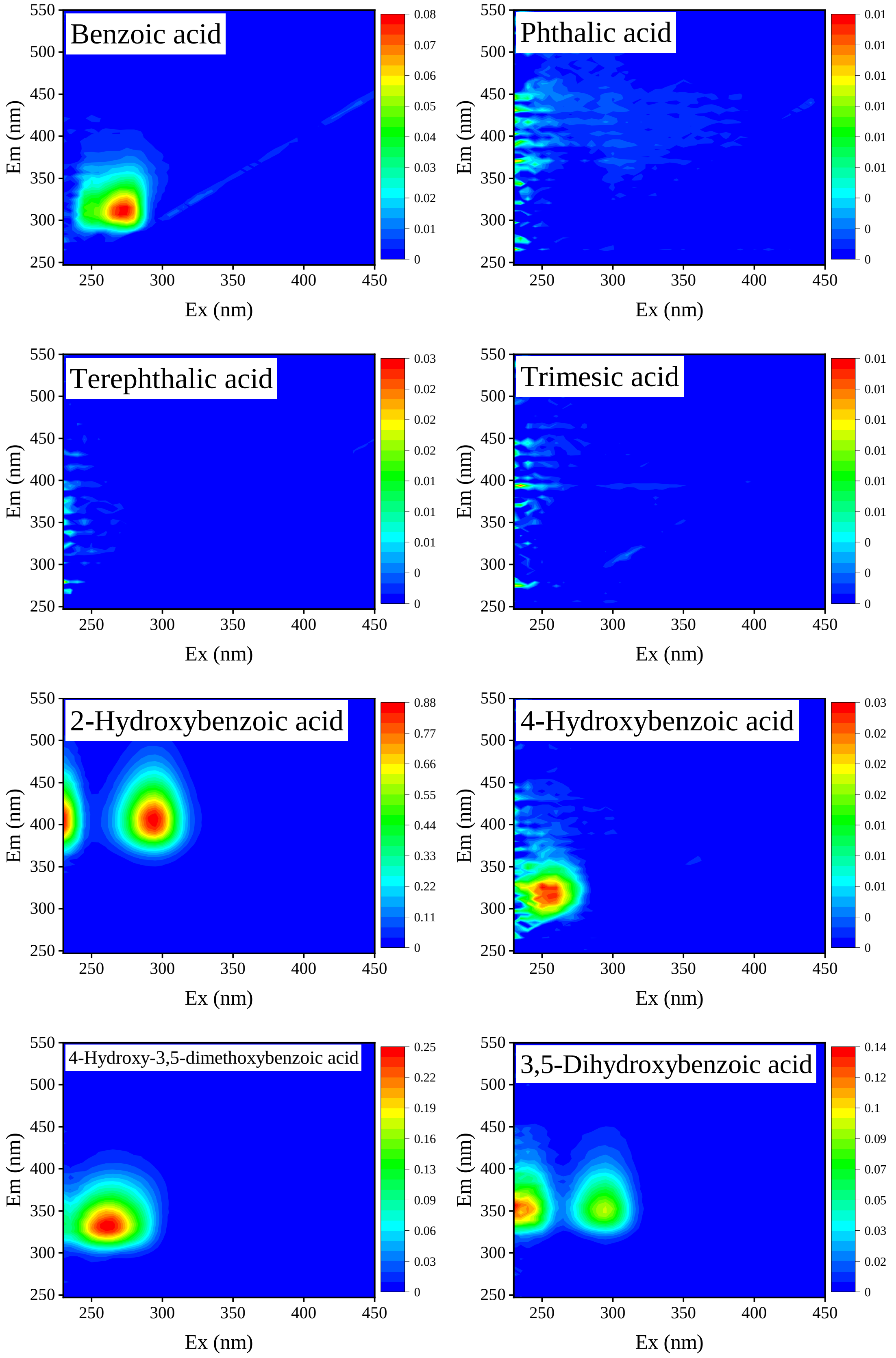

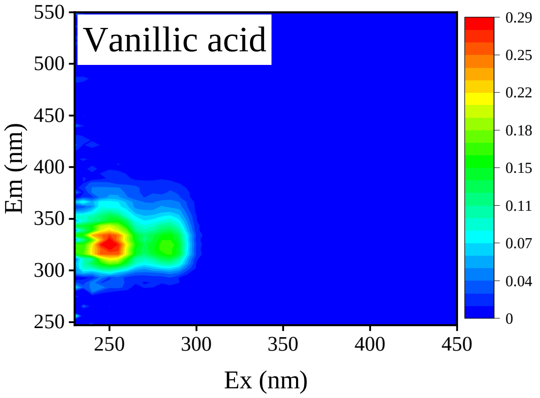

(c) Nitroaromatic compounds

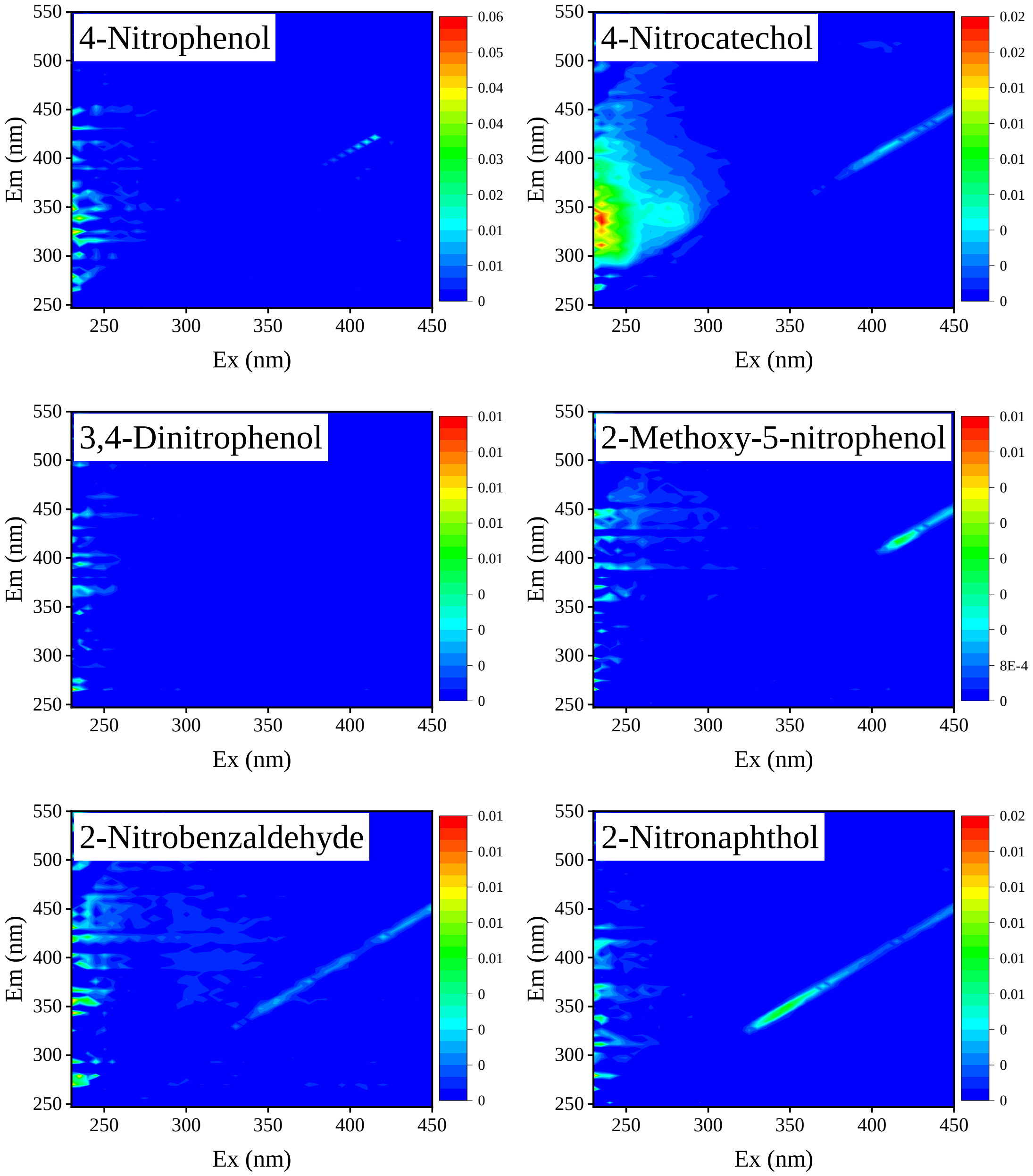

(d) Protein-like compounds

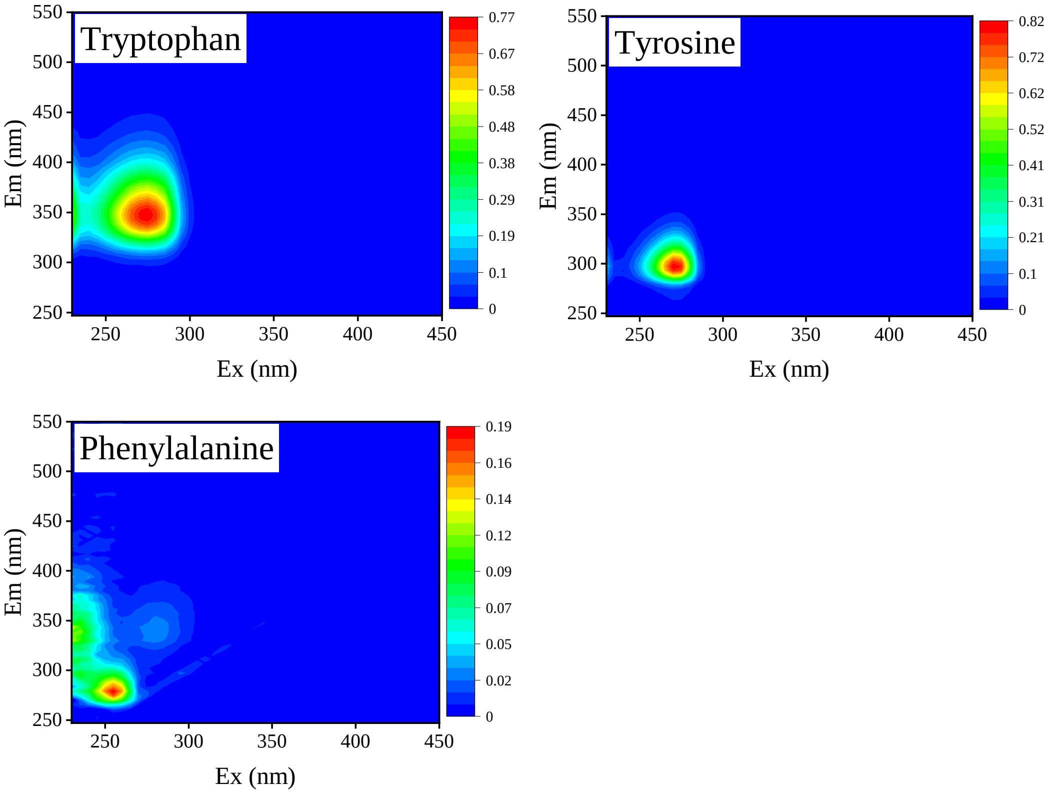

(e) N-heterocyclic compounds

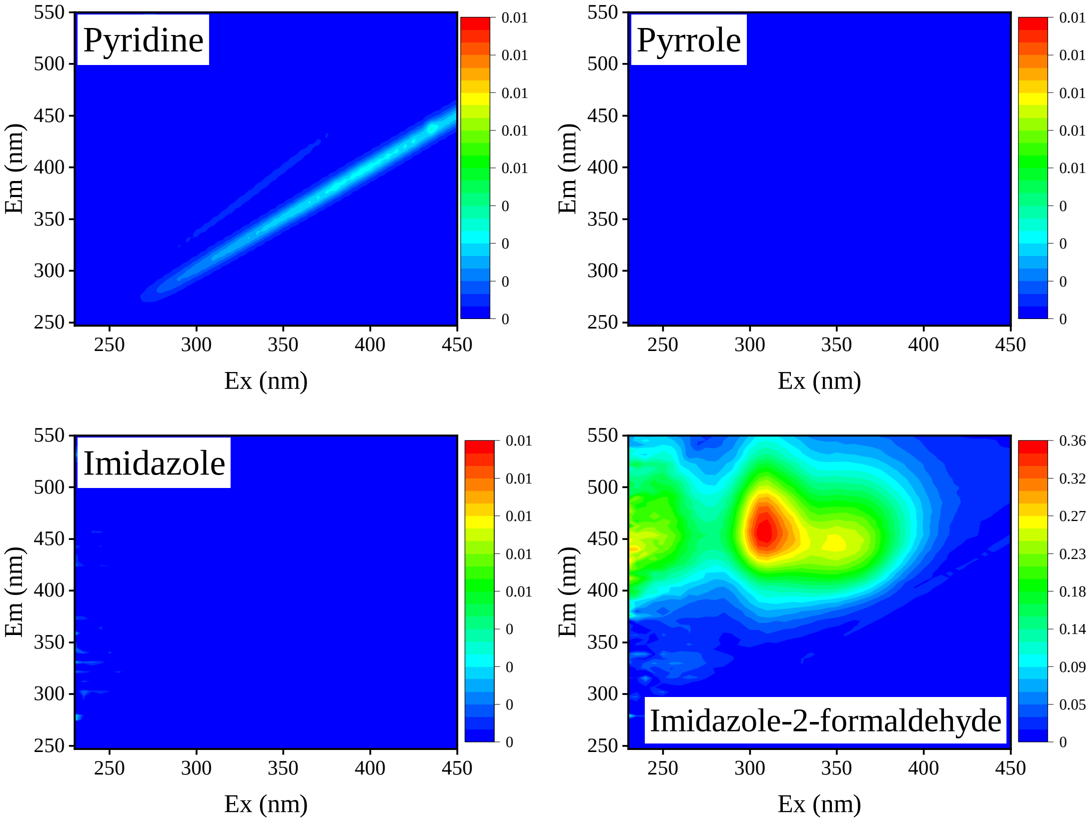

(f) Polycyclic aromatic hydrocarbons

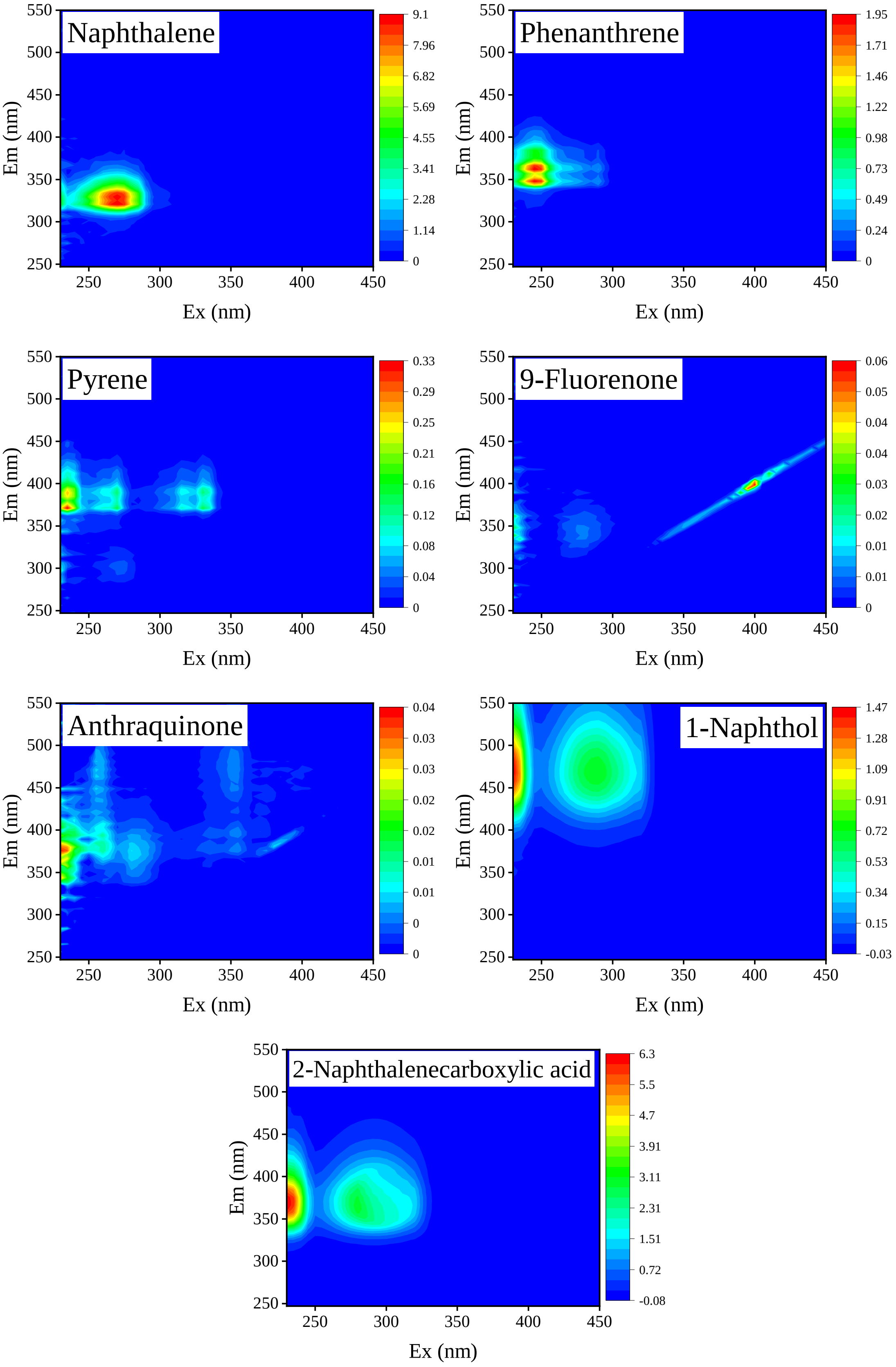

Figure S1. The 3D-EEM spectra of BrC model compounds

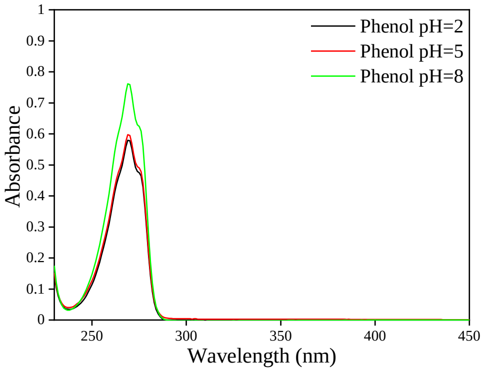
Absorbance
Wavelength (nm)
0
0.1
0.2
0.3
0.4
0.5
0.6
0.7
0.8
0.9
1
250
300
350
400
450
Phenol pH=2
Phenol pH=5
Phenol pH=8

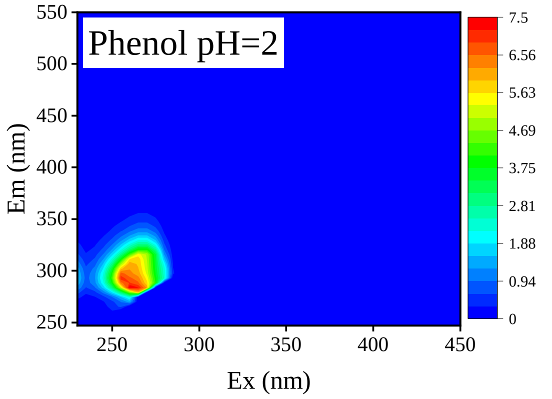
Phenol pH=2
Em (nm)
Ex (nm)
250
300
350
400
450
500
550
250
300
350
400
450
7.5
6.56
5.63
4.69
3.75
2.81
1.88
0.94
0

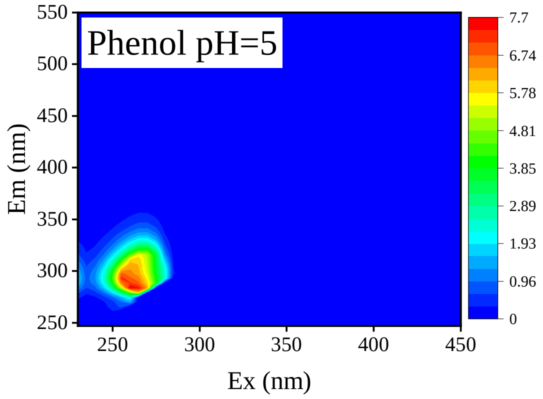
Phenol pH=5
Em (nm)
Ex (nm)
250
300
350
400
450
500
550
250
300
350
400
450
7.7
6.74
5.78
4.81
3.85
2.89
1.93
0.96
0

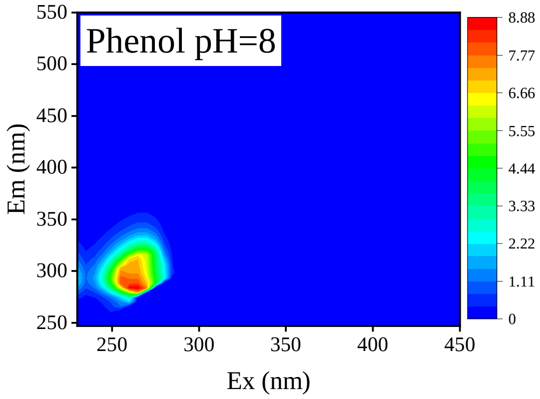
Phenol pH=8
Em (nm)
Ex (nm)
250
300
350
400
450
500
550
250
300
350
400
450
8.88
7.77
6.66
5.55
4.44
3.33
2.22
1.11
0

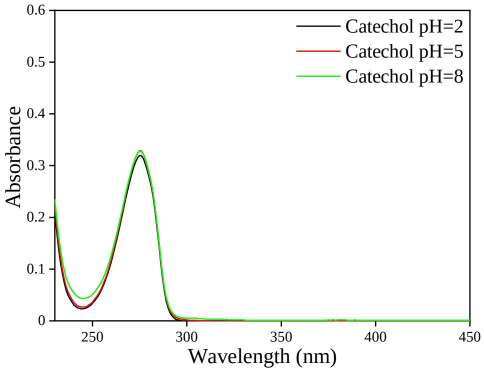
Absorbance
Wavelength (nm)
0
0.1
0.2
0.3
0.4
0.5
0.6
250
300
350
400
450
Catechol pH=2
Catechol pH=5
Catechol pH=8

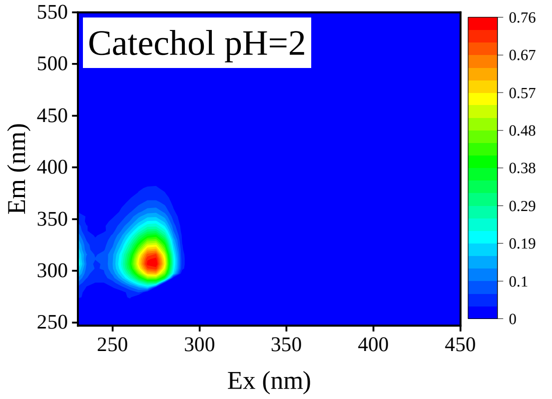
Catechol pH=2
Em (nm)
Ex (nm)
250
300
350
400
450
500
550
250
300
350
400
450
0.76
0.67
0.57
0.48
0.38
0.29
0.19
0.1
0

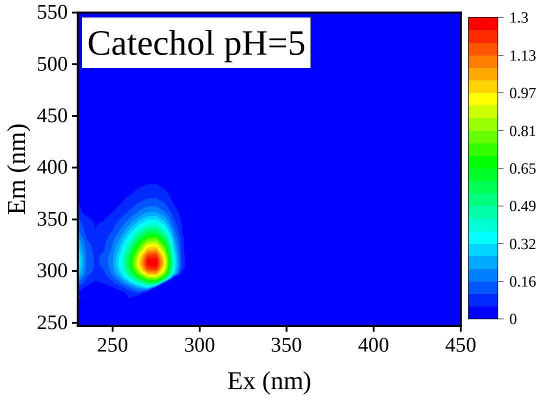
Catechol pH=5
Em (nm)
Ex (nm)
250
300
350
400
450
500
550
250
300
350
400
450
1.3
1.13
0.97
0.81
0.65
0.49
0.32
0.16
0

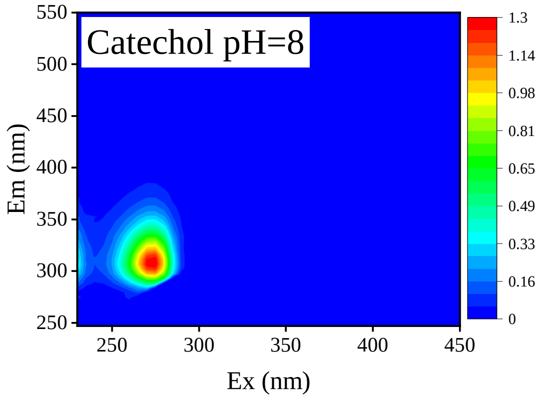
Catechol pH=8
Em (nm)
Ex (nm)
250
300
350
400
450
500
550
250
300
350
400
450
1.3
1.14
0.98
0.81
0.65
0.49
0.33
0.16
0

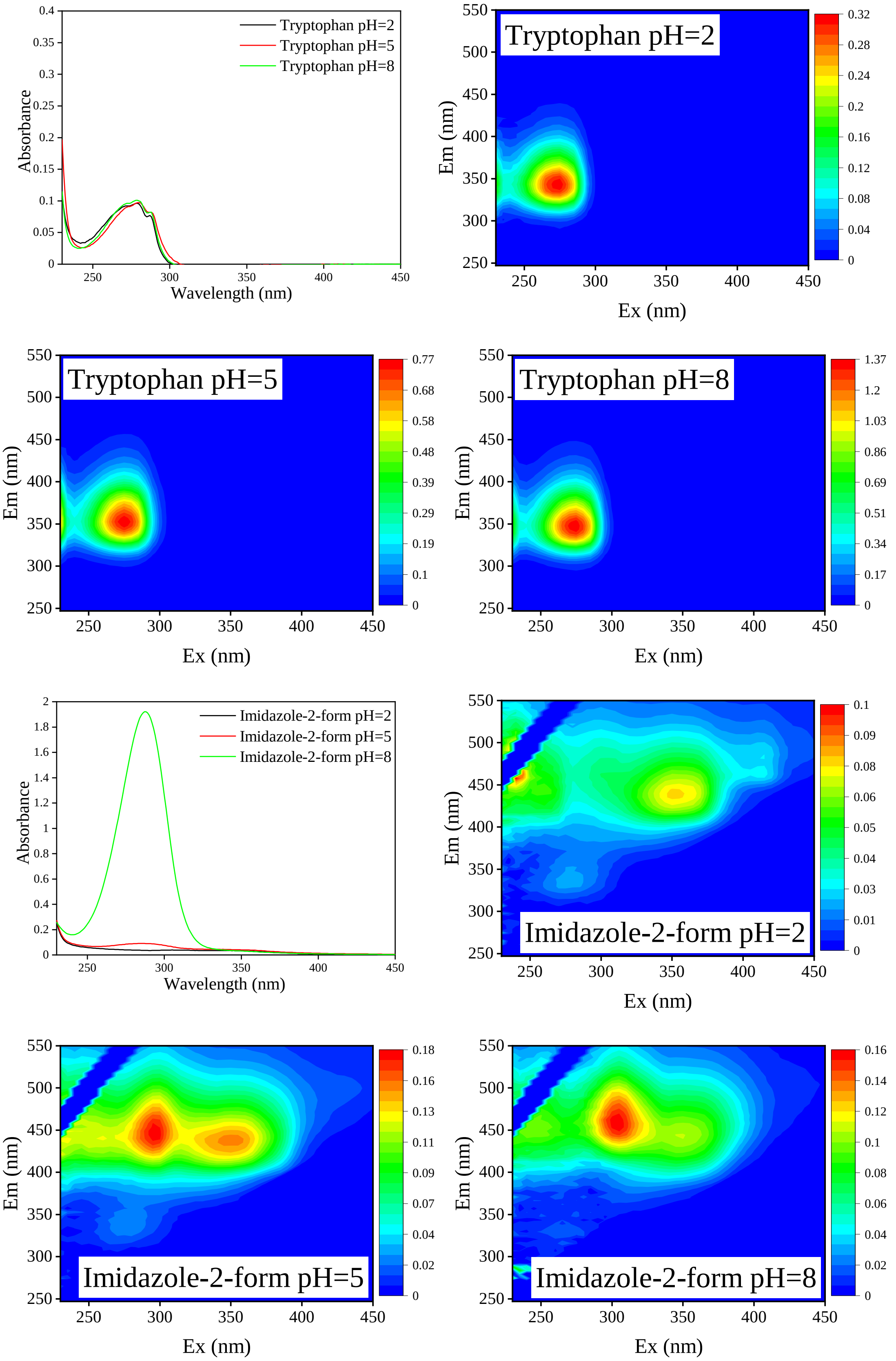

Figure S2. The normalized absorption spectra and 3D-EEM spectra of phenol, catechol, tryptophan and imidazole-2-formaldehyde measured at pH = 2, 5, and 8.

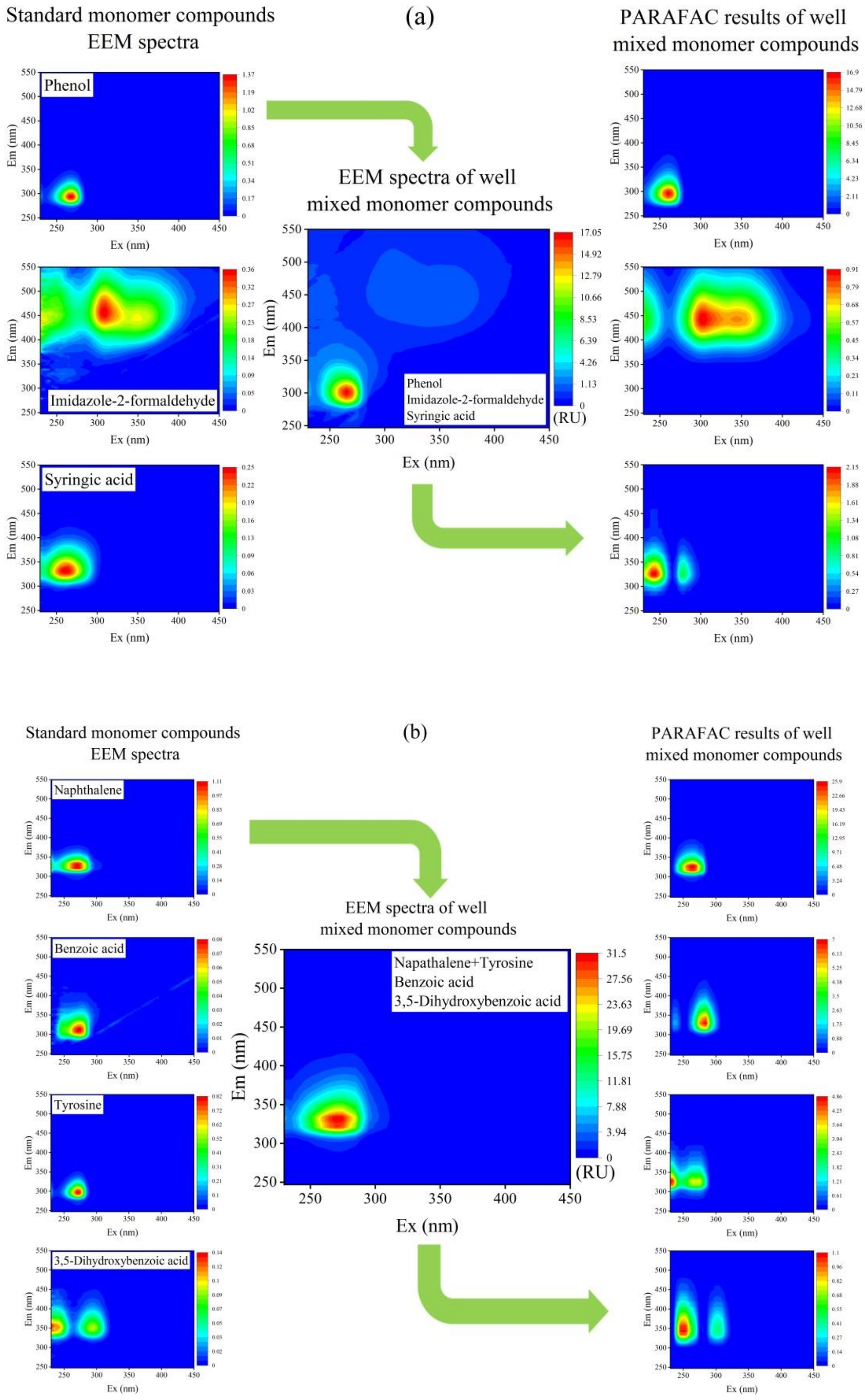

Figure S3. Fluorescence spectra of different monomer compounds after mixing and the fluorescent components obtained using PARAFAC (a, b represent different mixing samples).

(a) biomass burning

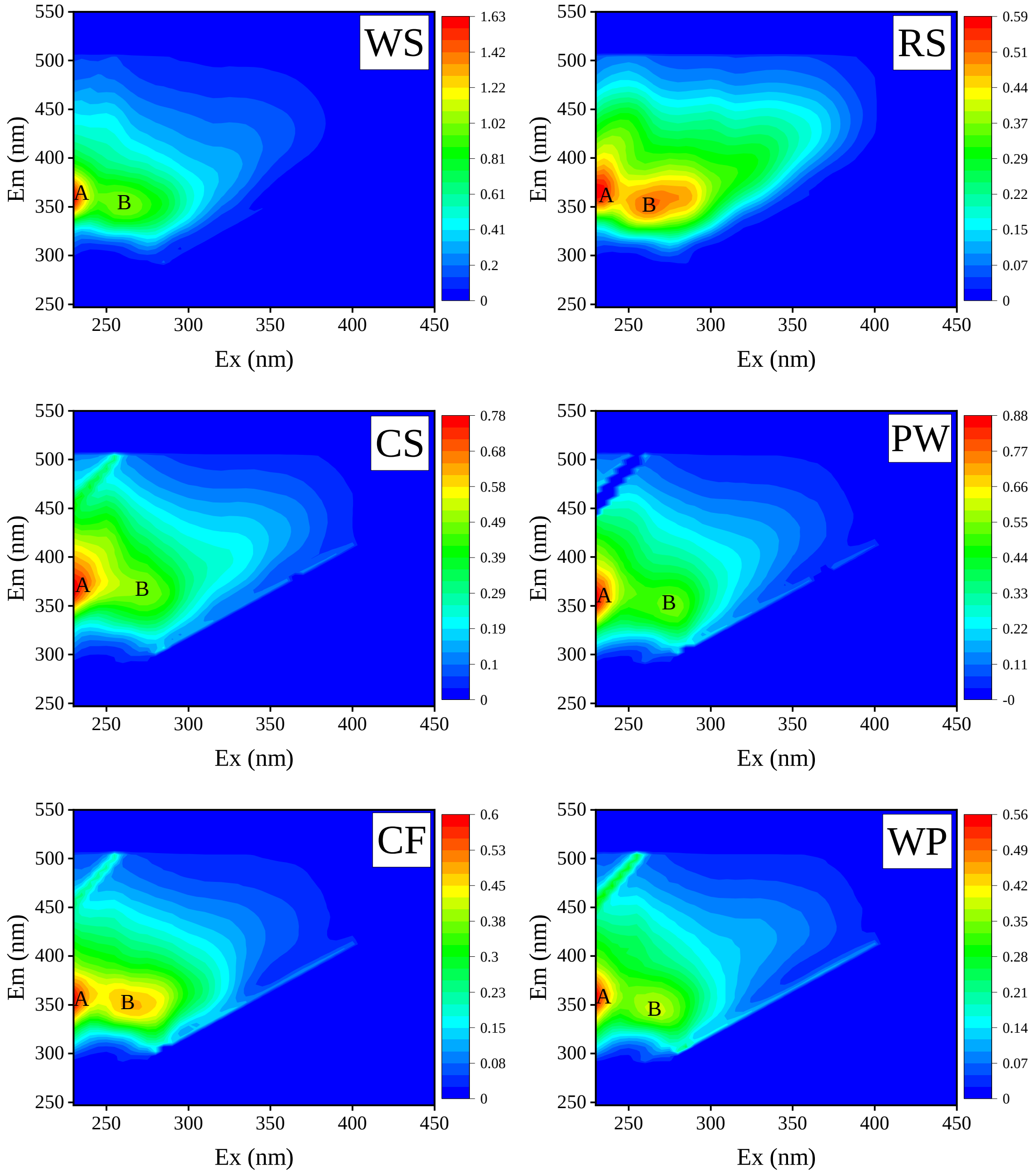

(b) coal combustion

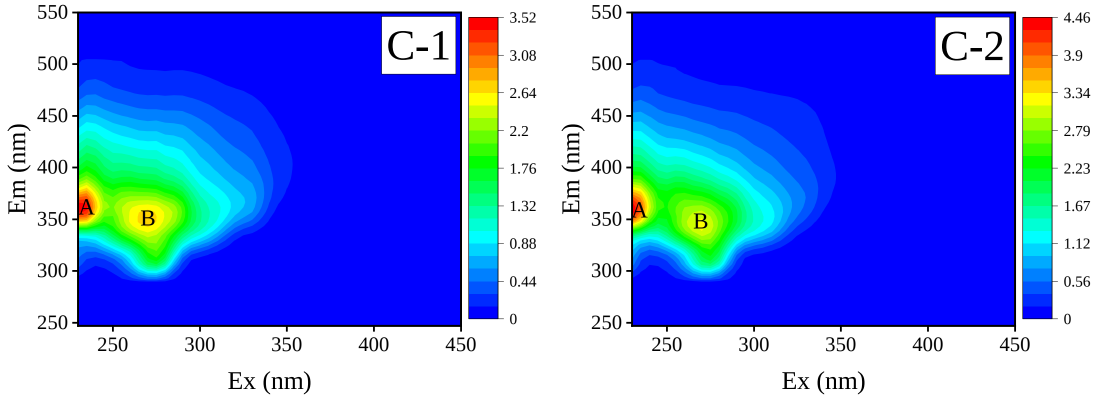

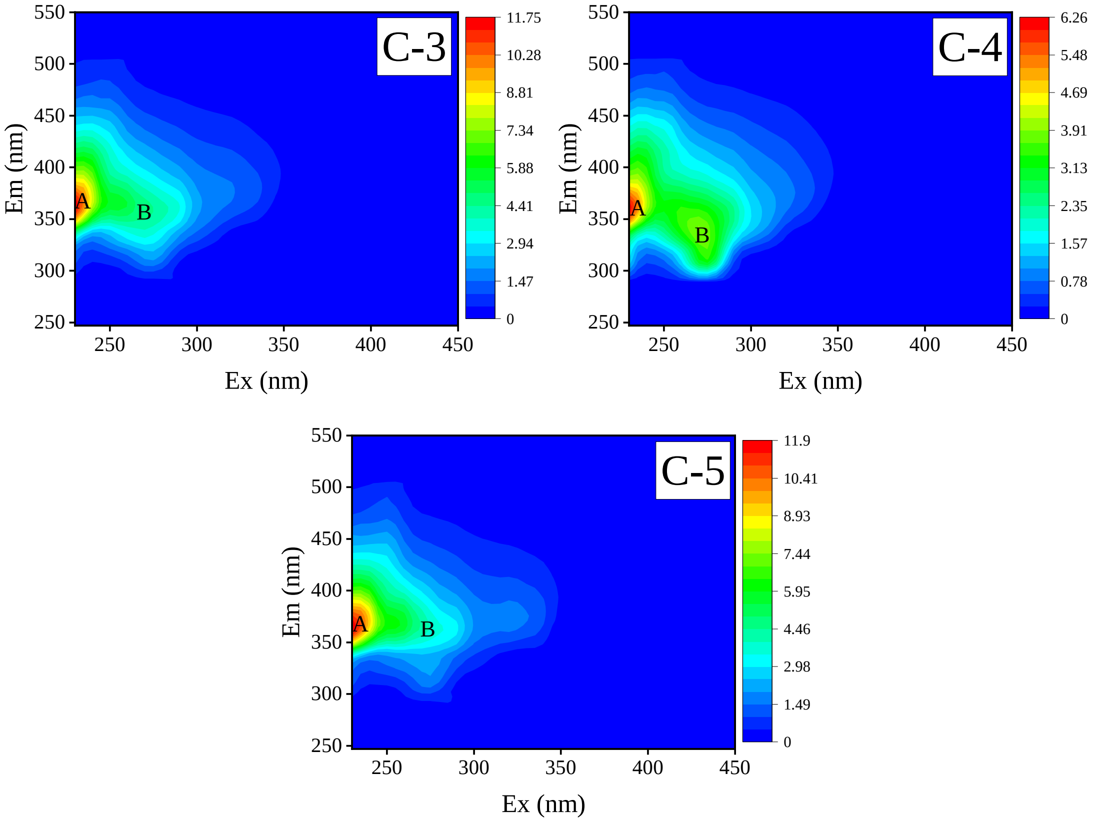

(c) vehicle emission

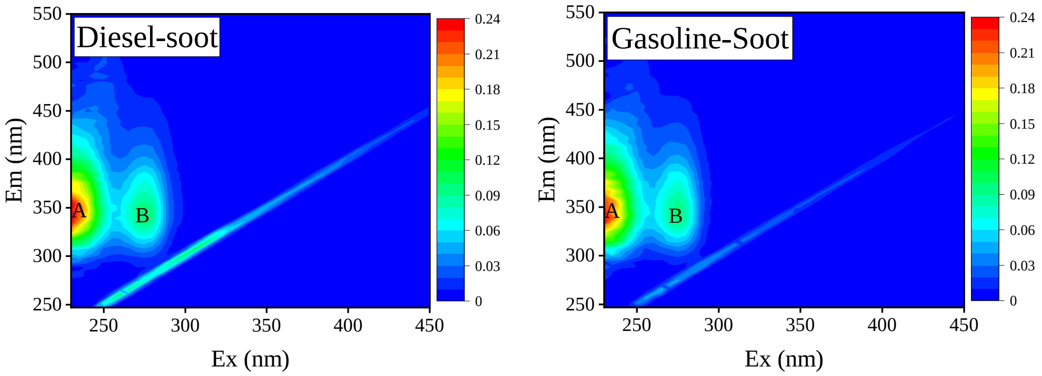

Figure S4. The 3D-EEM spectra of WSOM extracted from (a) biomass burning, (b) coal combustion, and (c) vehicle emission-derived particles.

(a) soil-derived DOM

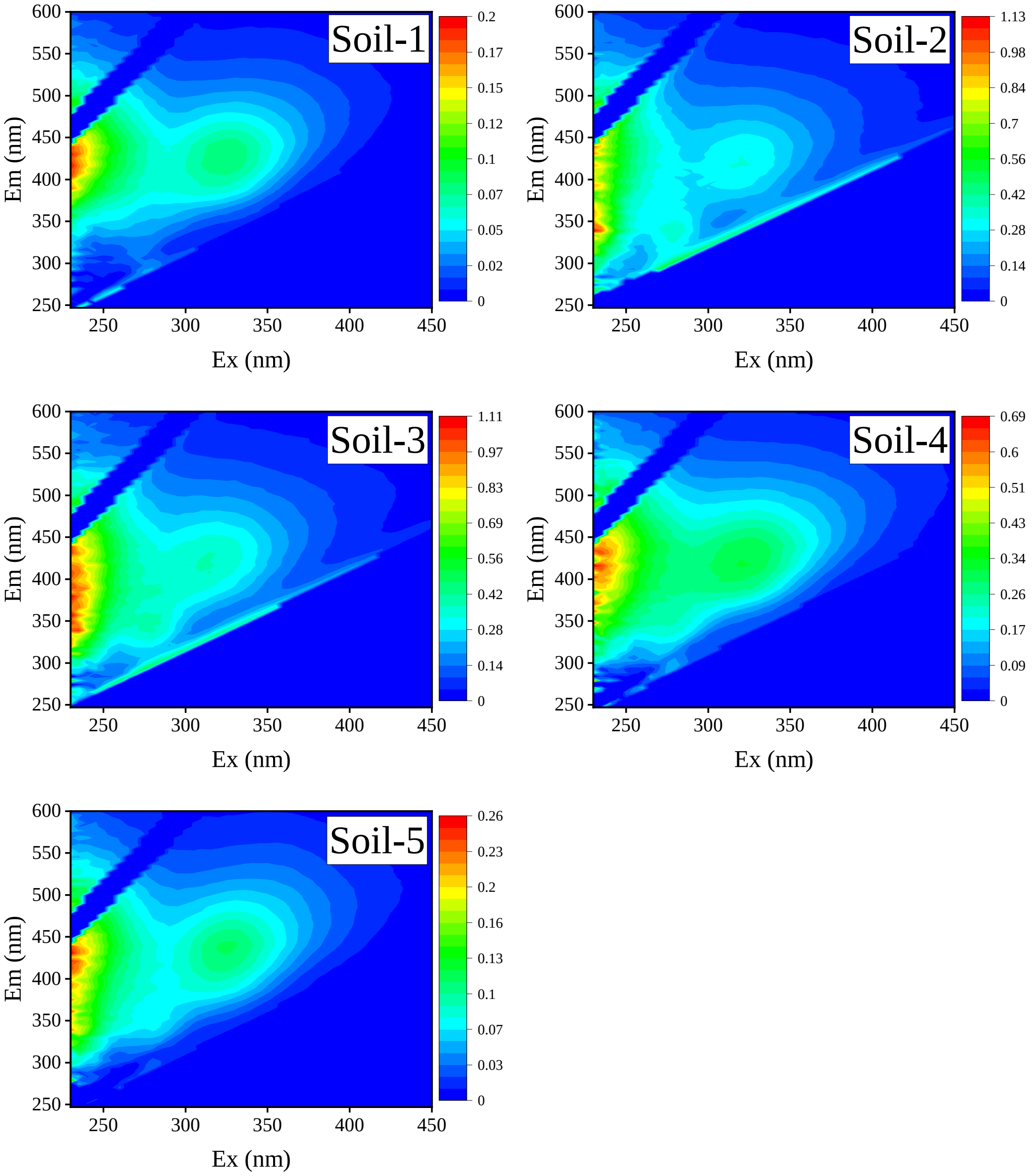

(b) FA and HA

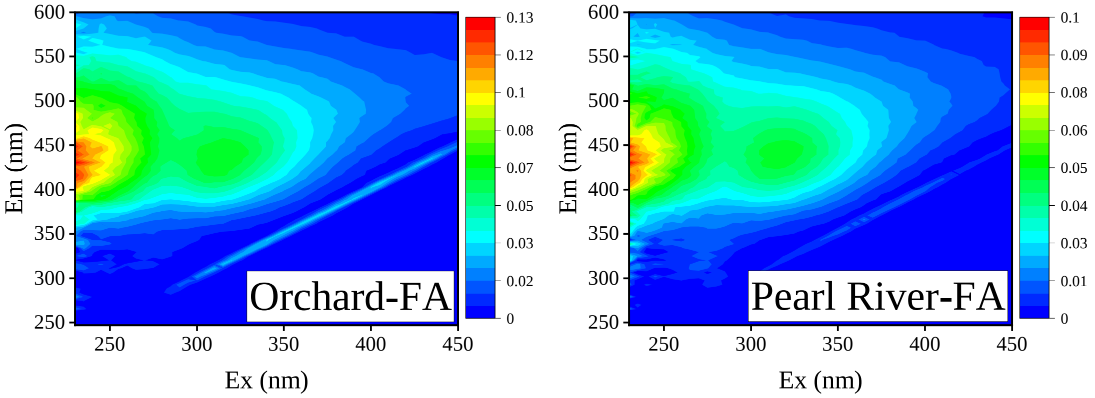

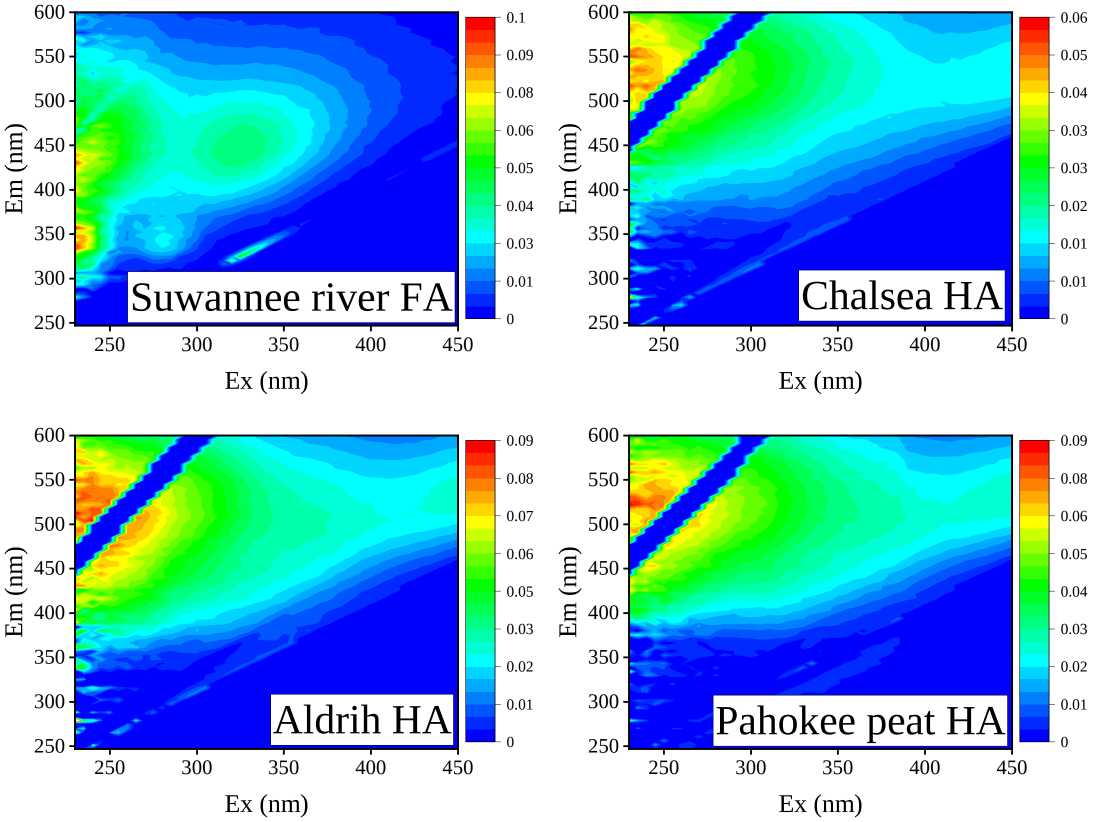

Figure S5. The 3D-EEM spectra of (a) soil DOM and (b) purified fulvic acid (FA) and humic acid (HA)

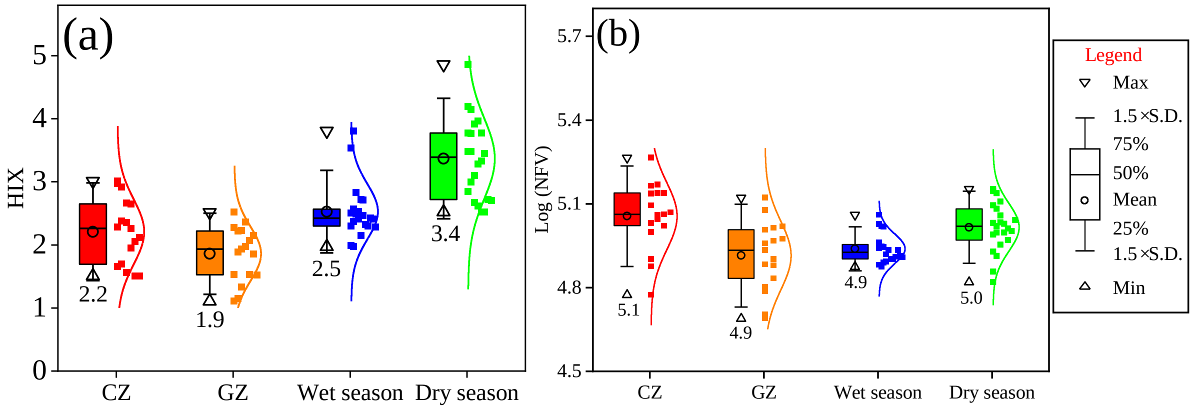

Figure S6. The HIX (a) and log(NFV) (b) value of WSOM of atmospheric aerosol particulate matter sampled at CZ and GZ in April 6-21, 2021 and wet and dry season at GZ in February 2018- January 2019.

References:

Ackendorf, J. M., Ippolito, M. G., and Galloway, M. M.: pH Dependence of the Imidazole-2-carboxaldehyde Hydration Equilibrium: Implications for Atmospheric Light Absorbance, Environ. Sci. Technol. Let., 4, 551-555, http://doi.org/10.1021/acs.estlett.7b00486, 2017.

Andrade-Eiroa, Á., Canle, M., and Cerdá, V.: Environmental Applications of Excitation-Emission Spectrofluorimetry: An In-Depth Review I, Appl. Spec. Rev., 48, 1-49, http://doi.org/10.1080/05704928.2012.692104, 2013.

Bai, Z., Zhang, L. Y., Cheng, Y., Zhang, W., Mao, J. F., Chen, H., Li, L., Wang, L. N., and Chen, J. M.: Water/Methanol-Insoluble Brown Carbon Can Dominate Aerosol-Enhanced Light Absorption in Port Cities, Environ. Sci. Technol., 54, 14889-14898, 2020.

Bianco, A., Minella, M., De Laurentiis, E., Maurino, V., Minero, C., and Vione, D.: Photochemical generation of photoactive compounds with fulvic-like and humic-like fluorescence in aqueous solution, Chemosphere, 111, 529-536, http://doi.org/10.1016/j.chemosphere.2014.04.035, 2014.

Bianco, A., Passananti, M., Deguillaume, L., Mailhot, G., and Brigante, M.: Tryptophan and tryptophan-like substances in cloud water: Occurrence and photochemical fate, Atmos. Environ., 137, 53-61, http://doi.org/10.1016/j.atmosenv.2016.04.034, 2016.

Cao, T., Li, M. J., Zou, C. L., Fan, X. J., Song, J. Z., Jia, W. L., Yu, C. L., Yu, Z. Q., and Ping, P. A.: Chemical composition, optical properties, and oxidative potential of water- and methanol-soluble organic compounds emitted from the combustion of biomass materials and coal, Atmos. Chem. Phys., 21, 13187-13205, http://doi.org/10.5194/acp-21-13187-2021, 2021.

Castells, P., Santos, F. J., and Gaiceran, M. T.: Development of a sequential supercritical fluid extraction method for the analysis of nitrated and oxygenated derivatives of polycyclic aromatic hydrocarbons in urban aerosols, J. Chromatogr. A, 1010, 141-151, 2003.

Chen, Q., Li, J., Hua, X., Jiang, X., Mu, Z., Wang, M., Wang, J., Shan, M., Yang, X., Fan, X., Song, J., Wang, Y., Guan, D., and Du, L.: Identification of species and sources of atmospheric chromophores by fluorescence excitation-emission matrix with parallel factor analysis, Sci. Total Environ., 718, 137322, http://doi.org/10.1016/j.scitotenv.2020.137322, 2020.

Chow, K. S., Huang, X. H. H., and Yu, J. Z.: Quantification of nitroaromatic compounds in atmospheric fine particulate matter in Hong Kong over 3 years: field measurement evidence for secondary formation derived from biomass burning emissions, Environ. Chem., 13, 665-673, 2016.

Coble, P. G.: Characterization of marine and terrestrial DOM in seawater using excitation emission matrix spectroscopy, Marin. Chem., 51, 325-346, http://doi.org/10.1016/0304-4203(95)00062-3, 1996.

Fan, X., Cao, T., Yu, X., Wang, Y., Xiao, X., Li, F., Xie, Y., Ji, W., Song, J., Peng, P., amp, apos, and an: The evolutionary behavior of chromophoric brown carbon during ozone aging of fine particles from biomass burning, Atmos. Chem. Phys., 20, 4593-4605, http://doi.org/10.5194/acp-20-4593-2020, 2020.

Fu, P., Kawamura, K., Chen, J., Qin, M., Ren, L., Sun, Y., Wang, Z., Barrie, L. A., Tachibana, E., Ding, A., and Yamashita, Y.: Fluorescent water-soluble organic aerosols in the High Arctic atmosphere, Sci. Rep., 5, 9845, http://doi.org/10.1038/srep09845, 2015.

Huang, R.-J., Yang, L., Shen, J., Yuan, W., Gong, Y., Ni, H., Duan, J., Yan, J., Huang, H., You, Q., and Li, Y. J.: Chromophoric Fingerprinting of Brown Carbon from Residential Biomass Burning, Environ. Sci. Technol.

Let., 9, 102-111, http://doi.org/10.1021/acs.estlett.1c00837, 2021.

Huang, R. J., Yang, L., Shen, J. C., Yuan, W., Gong, Y. Q., Guo, J., Cao, W. J., Duan, J., Ni, H. Y., Zhu, C. S., Dai, W. T., Li, Y. J., Chen, Y., Chen, Q., Wu, Y. F., Zhang, R. J., Dusek, U., O'Dowd, C., and Hoffmann, T.: Water-Insoluble Organics Dominate Brown Carbon in Wintertime Urban Aerosol of China: Chemical Characteristics and Optical Properties, Environ. Sci. Technol., 54, 7836-7847, 2020.

Ikemori, F., Nakayama, T., and Hasegawa, H.: Characterization and possible sources of nitrated mono- and di-aromatic hydrocarbons containing hydroxyl and/or carboxyl functional groups in ambient particles in Nagoya, Japan, Atmos. Environ., 211, 91-102, 2019.

Jiang, H., Frie, A. L., Lavi, A., Chen, J. Y., Zhang, H., Bahreini, R., and Lin, Y.-H.: Brown Carbon Formation from Nighttime Chemistry of Unsaturated Heterocyclic Volatile Organic Compounds, Environ. Sci. Tech. Let., 6, 184-190, http://doi.org/10.1021/acs.estlett.9b00017, 2019.

Kitanovski, Z., Cusak, A., Grgic, I., and Claeys, M.: Chemical characterization of the main products formed through aqueous-phase photonitration of guaiacol, Atmos. Meas. Tech., 7, 2457-2470, 2014.

Kosyakov, D. S., Ul'yanovskii, N. V., Latkin, T. B., Pokryshkin, S. A., Berzhonskis, V. R., Polyakova, O. V., and Lebedev, A. T.: Peat burning – An important source of pyridines in the earth atmosphere, Environ. Pollut., 266, 115109, http://doi.org/10.1016/j.envpol.2020.115109, 2020.

Lee, J.Y., Lane, D.A., Heo, J.B., Yi, S.M., and Kim, Y.P.: Quantification and seasonal pattern of atmospheric reaction products of gas phase PAHs in $PM_{2.5}$, Atmos. Environ., 55, 17-25, 2012.

Li, W. J., Wang, J. F., Qi, L., Yu, W. T., Nie, D. Y., Shi, S. S., Gu, C. X., Ge, X. L., and Chen, M. D.: Molecular characterization of biomass burning tracer compounds in fine particles in Nanjing, China, Atmos. Environ., 240, 2020.

Lian, X. F., Tang, G. G., Dao, X., Hu, X. D., Xiong, X., Zhang, G. H., Wang, Z. H., Cheng, C. L., Wang, X. F., Bi, X. H., Li, L., Li, M., and Zhou, Z.: Seasonal variations of imidazoles in urban areas of Beijing and Guangzhou, China by single particle mass spectrometry, Sci. Total Environ., 844, 2022.

Lin, P., Aiona, P. K., Li, Y., Shiraiwa, M., Laskin, J., Nizkorodov, S. A., and Laskin, A.: Molecular Characterization of Brown Carbon in Biomass Burning Aerosol Particles, Environ. Sci. Technol., 50, 11815-11824, http://doi.org/10.1021/acs.est.6b03024, 2016.

Lin, P., Bluvshtein, N., Rudich, Y., Nizkorodov, S. A., Laskin, J., and Laskin, A.: Molecular Chemistry of Atmospheric Brown Carbon Inferred from a Nationwide Biomass Burning Event, Environ. Sci. Technol., 51, 11561-11570, http://doi.org/10.1021/acs.est.7b02276, 2017.

Chow, K. S., Huang, X. H. H., and Yu, J. Z.: Quantification of nitroaromatic compounds in atmospheric fine particulate matter in Hong Kong over 3 years: field measurement evidence for secondary formation derived from biomass burning emissions, Environ Chem, 13, 665-673, 2016.

Mahamuni, G., Rutherford, J., Davis, J., Molnar, E., Posner, J. D., Seto, E., Korshin, G., and Novosselov, I.: Excitation–Emission Matrix Spectroscopy for Analysis of Chemical Composition of Combustion Generated Particulate Matter, Environ. Sci. Technol., 54, 8198-8209, http://doi.org/10.1021/acs.est.0c01110, 2020.

Matos, J. T. V., Freire, S. M. S. C., Duarte, R. M. B. O., and Duarte, A. C.: Natural organic matter in urban aerosols: Comparison between water and alkaline soluble components using excitation-emission matrix fluorescence spectroscopy and multiway data analysis, Atmos. Environ., 102, 1-10, http://doi.org/10.1016/j.atmosenv.2014.11.042, 2015.

Murphy, K. R., Stedmon, C. A., Graeber, D., and Bro, R.: Fluorescence spectroscopy and multi-way techniques. PARAFAC, Anal. Meth., 5, 6557, http://doi.org/10.1039/c3ay41160e, 2013.

Murphy, K. R., Timko, S. A., Gonsior, M., Powers, L. C., Wünsch, U. J., and Stedmon, C. A.: Photochemistry Illuminates Ubiquitous Organic Matter Fluorescence Spectra, Environ. Sci. Technol., 52, 11243-11250, http://doi.org/10.1021/acs.est.8b02648, 2018.

Qin, J., Zhang, L., Zhou, X., Duan, J., Mu, S., Xiao, K., Hu, J., and Tan, J.: Fluorescence fingerprinting properties for exploring water-soluble organic compounds in $PM_{2.5}$ in an industrial city of northwest China, Atmos. Environ., 184, 203-211, http://doi.org/10.1016/j.atmosenv.2018.04.049, 2018.

Santos, P.S.M., Cardoso, H.B., Rocha-Santos, T.A.P., and Duarte, A.C., Oxidation of benzoic acid from biomass burning in atmospheric waters, Environ. Pollut., 244, 693-704, 2019.

Sengupta, D., Samburova, V., Bhattarai, C., Watts, A. C., Moosmuller, H., and Khlystov, A. Y.: Polar semivolatile organic compounds in biomass-burning emissions and their chemical transformations during aging in an oxidation flow reactor, Atmos. Chem. Phys., 20, 8227-8250, 2020.

Sharp, J. R., Grace, D. N., Ma, S. Q., Woo, J. L., and Galloway, M. M.: Competing Photochemical Effects in Aqueous Carbonyl/Ammonium Brown Carbon Systems, Acs Earth Space Chem., 5, 1902-1915, 2021.

Shen, H., Chen, Z., Li, H., Qian, X., Qin, X., Shi, W.: Gas-Particle Partitioning of Carbonyl Compounds in the Ambient Atmosphere, Environ. Sci. Technol., 52, 10997-11006, 2018.

Smith, J.D., Sio, V., Yu, L., Zhang, Q., and Anastasio, C.: Secondary organic aerosol production from aqueous reactions of atmospheric phenols with an organic triplet excited state, Environ. Sci. Technol., 48, 1049-1057, 2014.

Song, T., Wang, S., Zhang, Y., Song, J., Liu, F., Fu, P., Shiraiwa, M., Xie, Z., Yue, D., Zhong, L., Zheng, J., and Lai, S.: Proteins and Amino Acids in Fine Particulate Matter in Rural Guangzhou, Southern China: Seasonal Cycles, Sources, and Atmospheric Processes, Environ. Sci. Technol., 51, 6773-6781, 2017.

Stedmon, C. A., and Bro, R.: Characterizing dissolved organic matter fluorescence with parallel factor analysis: a tutorial, Limn. Ocean Meth., 6, 572-579, 10.4319/lom.2008.6.572, 2008.

Tang, J., Li, J., Su, T., Han, Y., Mo, Y., Jiang, H., Cui, M., Jiang, B., Chen, Y., Tang, J., Song, J., Peng, P. a., and Zhang, G.: Molecular compositions and optical properties of dissolved brown carbon in biomass burning, coal combustion, and vehicle emission aerosols illuminated by excitation–emission matrix spectroscopy and Fourier transform ion cyclotron resonance mass spectrometry analysis, Atmos. Chem. Phys., 20, 2513-2532, http://doi.org/10.5194/acp-20-2513-2020, 2020a.

Teich, M., van Pinxteren, D., and Herrmann, H.: A one year study of functionalised medium-chain carboxylic acids in atmospheric particles at a rural site in Germany revealing seasonal trends and possible sources, J. Atmos. Chem., 76, 115-132, 2019.

Teich, M., van Pinxteren, D., Wang, M., Kecorius, S., Wang, Z., Müller, T., Močnik, G., and Herrmann, H.: Contributions of nitrated aromatic compounds to the light absorption of water-soluble and particulate brown carbon in different atmospheric environments in Germany and China, Atmos. Chem. Phys., 17, 1653-1672, 2017.

Vione, D., Albinet, A., Barsotti, F., Mekic, M., Jiang, B., Minero, C., Brigante, M., and Gligorovski, S.: Formation of substances with humic-like fluorescence properties, upon photoinduced oligomerization of typical phenolic compounds emitted by biomass burning, Atmos. Environ., 206, 197-207, http://doi.org/10.1016/j.atmosenv.2019.03.005, 2019.

Wang, X., Gu, R., Wang, L., Xu, W., Zhang, Y., Chen, B., Li, W., Xue, L., Chen, J., and Wang, W.: Emissions of fine particulate nitrated phenols from the burning of five common types of biomass, Environ. Pollut., 230, 405-412, 2017.

Yang, H.-H., Tsai, C.-H., Chao, M.-R., Su, Y.-L., and Chien, S.-M.: Source identification and size distribution of atmospheric polycyclic aromatic hydrocarbons during rice straw burning period, Atmos. Environ., 40, 1266-1274, 2006.

Yang, Y., Qin, Y., Qin, J., Zhou, X., Xv, P., Tan, J., and Xiao, K.: Facile Differentiation of Four Sources of Water-Soluble Organic Carbon in Atmospheric Particulates Using Multiple Fluorescence Spectral Fingerprints, Environ. Sci. Technol. Let., 9, 359-365, http://doi.org/10.1021/acs.estlett.2c00128, 2022.

Yu, L., Smith, J., Laskin, A., Anastasio, C., Laskin, J., and Zhang, Q.: Chemical characterization of SOA formed from aqueous-phase reactions of phenols with the triplet excited state of carbonyl and hydroxyl radical, Atmos. Chem. Phys., 14, 13801-13816, http://doi.org/10.5194/acp-14-13801-2014, 2014.

Yu, L., Smith, J., Laskin, A., George, K. M., Anastasio, C., Laskin, J., Dillner, A. M., and Zhang, Q.: Molecular transformations of phenolic SOA during photochemical aging in the aqueous phase: competition among oligomerization, functionalization, and fragmentation, Atmos. Chem. Phys., 16, 4511-4527, http://doi.org/10.5194/acp-16-4511-2016, 2016.

Yuan, W., Huang, R.-J., Yang, L., Guo, J., Chen, Z., Duan, J., Wang, T., Ni, H., Han, Y., Li, Y., Chen, Q., Chen, Y., Hoffmann, T., and O'Dowd, C.: Characterization of the light-absorbing properties, chromophore composition and sources of brown carbon aerosol in Xi'an, northwestern China, Atmos. Chem. Phys., 20, 5129-5144, 2020.

Zhang, L., Yang, L., Bi, J., Liu, Y., Toriba, A., Hayakawa, K., Nagao, S., Tang, N.: Characteristics and unique sources of polycyclic aromatic hydrocarbons and nitro-polycyclic aromatic hydrocarbons in $PM_{2.5}$ at a highland background site in northwestern China, Environ. Pollut., 274, 116527, 2021.

Zhang, Q. and Anastasio, C.: Free and combined amino compounds in atmospheric fine particles ($PM_{2.5}$) and fog waters from Northern California, Atmos. Environ., 37, 2247-2258, 2003.